TABLE I
AVERAGE PERCENT DEVIATION BETWEEN THE MEASURED DISPERSION AND THE MODELS LISTED IN THE REFERENCES

ϵ_r	Thickness	Z_0	[3]	[4]	[5]	[6]	[7]	[8]	[2]	[9]	[10]
9.80	0.655 mm	50Ω	0.51	0.37	1.56	3.14	1.27	0.70	**0.34**	1.41	1.91
9.80	0.655 mm	50Ω	**0.47**	0.55	1.38	2.95	1.69	0.76	0.62	1.83	2.32
9.80	0.648 mm	35Ω	0.38	**0.28**	1.46	3.07	0.94	1.06	0.69	1.85	3.80
9.80	0.648 mm	50Ω	0.39	**0.32**	1.39	2.92	1.50	0.77	0.43	1.69	2 23
9.80	0.648 mm	70Ω	0.56	**0.55**	1.35	3.00	1.89	0.95	0.65	1.44	0.84
9.80	0.668 mm	50Ω	**0.58**	0.84	1.13	2.71	1.99	0.69	0.95	2.16	2 69
9.80	0.668 mm	50Ω	0.54	0.67	1.04	2.54	1.84	**0.51**	0.74	1.95	2.45
9.80	0.635 mm	50Ω	**0.31**	0.32	1.31	2.95	1.60	0.78	0.47	1.80	2.24
9.80	0.635 mm	70Ω	**0.32**	0.32	1.17	2.80	1.81	0.69	0.41	1.50	1.10
2.20	1.605 mm	50Ω	0.56	**0.51**	0.65	1.18	1.99	2.57	0.78	1.87	2 67
2.20	1.605 mm	70Ω	0.52	0.54	0.41	0.88	1.24	2.49	**0.45**	1.61	2.50
2.20	0.780 mm	50Ω	0.56	0.58	0.54	0.48	0.68	1.01	0.53	**0.39**	1.67
2.20	0.780 mm	70Ω	0.53	0.53	0.56	**0.50**	0.56	1.01	0.76	0.51	0 98
2.33	1.524 mm	50Ω	0.48	0.46	0.50	**0.45**	0.81	1.28	0.61	0.99	1.51
2.33	1.524 mm	35Ω	0.46	**0.43**	0.59	0.51	0.77	1.12	0.86	1.17	1.21
2.17	0.686 mm	50Ω	**0.41**	0.42	0.52	0.41	0.80	1.02	0.75	0.50	1.14
2.33	0.787 mm	50Ω	0.53	0.55	0.57	0.45	0.78	1.10	0.71	**0.44**	1.59
2.50	0.762 mm	50Ω	**0.23**	0.27	0.47	0.41	0.71	1.14	0.63	0.37	1.50

The results for 18 different resonators are given, and the smallest deviation for each case is highlighted

models gave the most consistent results for the substrates ($2.2 \leqslant \epsilon_r \leqslant 9.8$) and line impedances ($35\ \Omega \leqslant \epsilon_r \leqslant 75\ \Omega$) that were tested. Caution should be exercised in extrapolating these conclusions to substrates and line widths outside this range [13].

REFERENCES

[1] H. A Atwater, "Tests of microstrip dispersion formulas," *IEEE Trans. Microwave Theory Tech.*, vol. 36, pp. 619–621, Mar. 1988

[2] T. C. Edwards and R. P. Owens, "2–18 GHz dispersion measurements on 10–100 Ω microstrip lines on sapphire," *IEEE Trans. Microwave Theory Tech.*, vol MTT-24, pp. 506–513, Aug. 1976.

[3] M. Kirschning and R. H. Jansen, "Accurate model for effective dielectric constant with validity up to millimeter-wave frequencies," *Electron. Lett.*, vol. 18, pp. 272–273, Jan. 1982

[4] M Kobayashi, "A dispersion formula satisfying recent requirements in microstrip CAD," *IEEE Trans. Microwave Theory Tech.*, vol. 36, pp. 1246–1250, Aug. 1988.

[5] E. Yamashita, K. Atsuki, and T. Ueda, "An accurate dispersion formula of microstrip lines for computer-aided design of microwave integrated circuits," *IEEE Trans. Microwave Theory Tech.*, vol. MTT-27, pp. 1036–1038, Dec 1979.

[6] E. Hammerstad and O. Jensen, "Accurate models for microstrip computer aided design," in *1980 IEEE MTT-S Int. Microwave Symp. Dig.* (Washington), pp. 407–409.

[7] P. Pramanick and P. Bhartia, "An accurate description of dispersion in microstrip," *Microwave J.*, pp 89–92, Dec 1983.

[8] W. J. Getsinger, "Microstrip dispersion model," *IEEE Trans. Microwave Theory Tech.*, vol MTT-21, pp. 34–39, Jan. 1973.

[9] H. J. Carlin, "A simplified circuit model for microstrip," *IEEE Trans. Microwave Theory Tech.*, vol. MTT-21, pp. 589–591, Sept. 1973.

[10] M V. Schneider, "Microstrip dispersion," *Proc. IEEE*, vol. 60, pp. 144–146, Jan 1972.

[11] E. J Denlinger, "A frequency dependent solution for microstrip transmission lines," *IEEE Trans. Microwave Theory Tech.*, vol MTT-19, pp. 30–39, Jan. 1971.

[12] R. A. York, "Microwave measurement of substrate dielectric constant and microstrip dispersion," master's thesis, Cornell University, Ithaca, NY, Aug 1989.

[13] R. L. Veghte and C. A Balanis, "Dispersion of transient signals in microstrip transmission lines," *IEEE Trans. Microwave Theory Tech.*, vol. MTT-34, pp 1427–1436, Dec. 1986.

A New Wire Node for Modeling Thin Wires in Electromagnetic Field Problems Solved by Transmission Line Modeling

P. NAYLOR AND C. CHRISTOPOULOS

***Abstract*—A new three-dimensional wire node for the numerical solution of electromagnetic field problems by transmission line modeling has been developed. The wire node can represent thin wires in a coarse mesh, thus substantially increasing computational efficiency. The scattering matrix for the node is given, together with a simulation result and comparisons with another method.**

I. INTRODUCTION

Transmission line modeling (TLM) has been applied extensively to the solution of electromagnetic field, diffusion, and network problems [1]. The use of TLM results in algorithms which are easy to understand and can be efficiently implemented. Knowledge of the electromagnetic fields inside structures such as aircraft and vehicles is useful for EMC studies. Usually of more interest is the calculation of voltages and currents induced on thin wires or antennas within such structures.

In practical cases the small size of these wires and the close proximity of metal boundaries can make the modeling of such a

Manuscript received January 17, 1989; revised October 5, 1989. This work was supported by the U K. Ministry of Defence (Procurement Executive)

The authors are with the Department of Electrical and Electronic Engineering, University of Nottingham, University Park, Nottingham, NG7 2RD, United Kingdom.

IEEE Log Number 8933243

geometry difficult. Various techniques have been used within TLM models to cope with such geometries, and these have been termed separated, integrated, and diakoptic solutions [2].

Integrated techniques model the wire within the field solution by short-circuiting selected nodes or transmission lines, but only at certain discrete points. The advantage of this technique over the separated solutions is that reradiation effects are modeled automatically. However, a fine mesh is required to model a thin wire accurately. The use of a fine mesh is generally not practical in that large computer resources are required. The simplest integrated wire model available is the short-circuit node [2], but this has poor propagational characteristics and a large, fixed radius relative to the nodal spacing. Separated solutions compute only approximate results, and the diakoptic methods present difficulties when using time and space approximations.

A new TLM node is required which allows the integrated modeling of wires of small radii but without the disadvantages associated with the short-circuit node.

II. The Wire Node

The new node reported here is a development of the symmetrical condensed node already used successfully in TLM [3], [4]. The wire node explicitly includes in its scattering properties the effects of a wire passing through the node along one of the coordinate directions, as shown for the Z direction in Fig. 1. Along the Z direction energy is distributed between the standard modes (lines 2, 4, 8, 9) and the new "common mode" (lines 13 and 14). Stubs have been introduced into the symmetrical condensed node [4] and the new lines 13 and 14 may also be regarded as a pseudostub. The common mode represented by lines 13 and 14 models the wirelike properties within the node. As with the symmetrical condensed node, a physical network is not available and the scattering matrix of the wire node has to be determined from Maxwell's equations and conservation of charge and energy. The latter condition requires, for a lossless junction, that the scattering matrix $\underline{S}$ be unitary [5]:

$$\underline{S}^T\underline{Y}\underline{S}=\underline{Y} \tag{1}$$

where $\underline{Y}$ is the admittance matrix of the transmission lines.

From these considerations $\underline{S}$ can be obtained and is

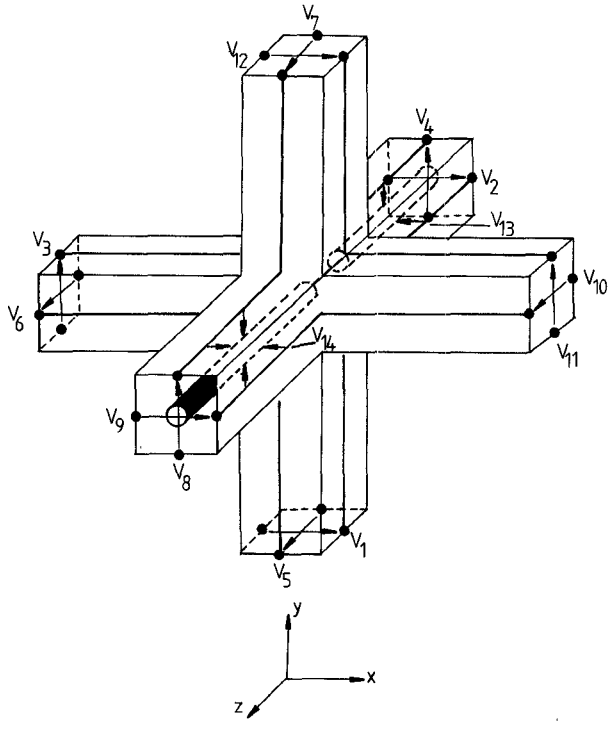

Fig. 1. TLM symmetrical condensed node with wire (wire node).

The admittance of the common-mode lines can be computed using the standard formula for a wire within a square coaxial cavity:

$$Y_{\text{cm}}=\frac{\sqrt{\epsilon_r}}{60\ln(0{\cdot}54\Delta l/r)} \tag{3}$$

where Δl is the internodal spacing and r is the wire radius. Y in (2) is set equal to $2Y_{\text{cm}}/Y_0$, where Y_0 is the admittance of free space.

Such a new code can be used in a very coarse TLM mesh to model a thin wire.

III. Results and Discussion

To confirm that the new wire node can model thin wires (that is, wires with a radius much smaller than the nodal spacing Δl), the geometry shown in Fig. 2 was modeled in two different ways.

$$\underline{S}=\begin{array}{c|cccccccccccccc}
 & 1 & 2 & 3 & 4 & 5 & 6 & 7 & 8 & 9 & 10 & 11 & 12 & 13 & 14 \\
\hline
1 & & 0.5 & 0.5 & & & & & & 0.5 & & -0.5 & & & \\
2 & 0.5 & & & & & 0.5 & & & & -0.5 & & 0.5 & & \\
3 & 0.5 & & & 0.5 & & & & 0.5 & & & & -0.5 & & \\
4 & & & 0.5 & & 0.5 & & -0.5 & & & & 0.5 & & & \\
5 & & & & 0.5 & $-a$ & b & $-a$ & -0.5 & & b & & & Yb & Yb \\
6 & & 0.5 & & & b & $-a$ & b & & -0.5 & $-a$ & & & Yb & Yb \\
7 & & & & -0.5 & $-a$ & b & $-a$ & 0.5 & & b & & & Yb & Yb \\
8 & & & 0.5 & & -0.5 & & 0.5 & & & & 0.5 & & & \\
9 & 0.5 & & & & & -0.5 & & & & 0.5 & & 0.5 & & \\
10 & & -0.5 & & & b & $-a$ & b & & 0.5 & $-a$ & & & Yb & Yb \\
11 & -0.5 & & & 0.5 & & & & 0.5 & & & & 0.5 & & \\
12 & & 0.5 & -0.5 & & & & & & 0.5 & & 0.5 & & & \\
13 & & & & & b & b & b & & & b & & & Yb & $-2b$ \\
14 & & & & & b & b & b & & & b & & & $-2b$ & Yb
\end{array} \tag{2}$$

$$a=\frac{Y}{2(Y+2)}, \qquad b=\frac{1}{Y+2}.$$

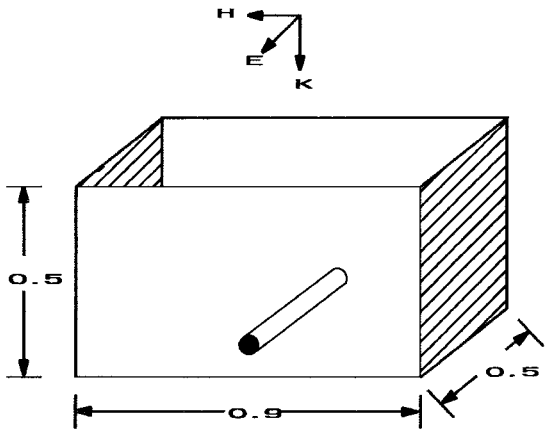

Fig. 2. Open box geometry. Dimensions in meters, hatched lines indicate open-circuit boundaries.

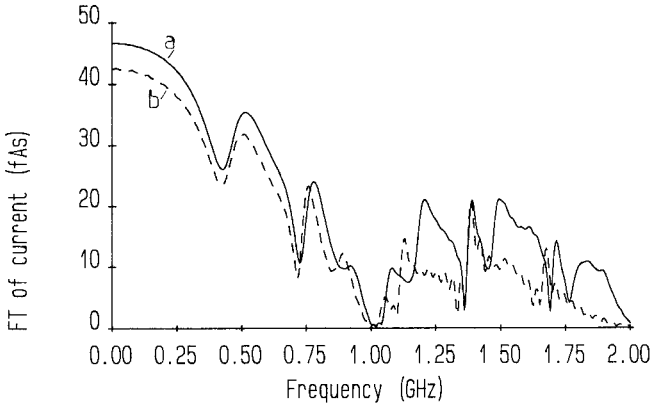

Fig. 3. Comparison of the frequency spectra for the geometry of Fig. 2 using *a*) fine mesh and *b*) wire node.

First, a fine mesh ($45\times25\times25$ nodes) model of this geometry was constructed using the ordinary symmetrical, condensed node, where the wire was modeled in the normal way by short-circuiting the transmission lines at a distance $\Delta l/2$ from the wire center. This is a slightly more accurate model than the short-circuit node mentioned in Section I and, for the problem under consideration, models an effective wire radius of 0.011 m.

Second, exactly the same problem was modeled using a coarse mesh of $9\times5\times5$ nodes. In this case a wire of radius 0.011 m cannot be described by short-circuiting nodes, as the nodal distance is too large ($\Delta l = 0.1$ m). For this reason, the thin wire was modeled using the new wire node. Substituting $r = 0.011$ m in (3) gives the admittance and hence the scattering matrix of the wire node.

Both numerical models of the problem were subjected to a plane wave impulse excitation as shown in Fig. 2. Results for the wire current obtained from the two models are compared in Fig. 3 (frequency response) and Fig. 4 (impulse response). Solid lines are for the conventional model using fine mesh and short-circuited nodes to model the wire. Broken lines are for the coarse mesh and the new wire node modeling the wire. Considering the differences in the modeling approach in the two cases, the agreement is excellent up to 1 GHz. This suggests that the wire node can accurately model thin wires ($r \ll \Delta l$). Agreement above approximately 1 GHz is less good, but this is not due to the properties of the wire node. It is due to a general deterioration in

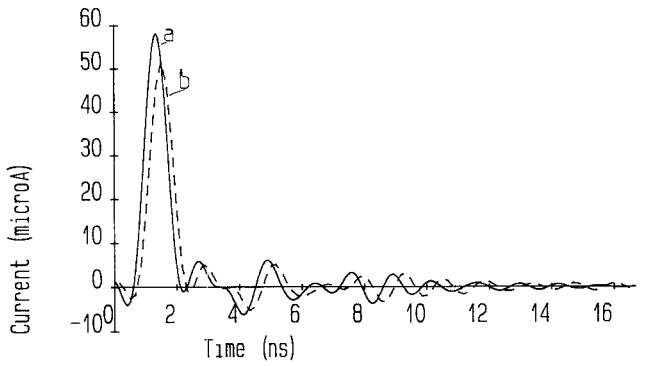

Fig. 4. Comparison of the time-domain response for the geometry of Fig. 2 Filtered to 1 GHz using *a*) fine mesh and *b*) wire node.

accuracy in modeling the field problem, as the number of nodes per wavelength is too small above this frequency.

The use of the wire node results in enormous benefits. For the example given, there is a 1/625 saving in computer execution time and a 1/125 saving in storage with little loss in accuracy.

At present only wires at the center of the node have been modeled. It should be possible in the future, using this technique, to model thin wires, off-center and multiconductor wires provided the scattering matrix can be calculated.

The wire node marks an important development in TLM, as it makes possible the description of thin wires within a coarse mesh, thus offering substantial savings in computer storage and run time.

Work is in progress to study the behavior of the wire node in different configurations, especially near terminations.

ACKNOWLEDGMENT

The authors wish to acknowledge the contribution to this work made by the late Professor P. B. Johns.

REFERENCES

[1] P. B. Johns, "The art of modeling," *IEEE Electron and Power*, pp. 565–569, Aug. 1979.
[2] P. Naylor, C. Christopoulos, and P. B. Johns, "Coupling between electromagnetic field and wires using transmission-line modelling," *Proc. Inst Elec. Eng.*, vol. 134, pt A, no. 8, pp. 679–686, Sept. 1987.
[3] P. B. Johns, "New symmetrical condensed node for three-dimensional solution of electromagnetic-wave problems by TLM," *Electron Lett.*, vol. 22, no. 3, pp. 162–164, Jan 1986.
[4] P. B. Johns, "A symmetrical condensed node for the TLM method," *IEEE Trans. Microwave Theory Tech.*, vol. MTT-35, pp. 370–377, Apr 1987.
[5] R. E. Collin, *Foundations for Microwave Engineering*. New York: McGraw-Hill, 1966.

Anisotropic Measurements of Rubber Sheets with an *X*-Band Three-Wave Interferometer

RENÉ SARDOS, JEAN-FRANÇOIS ESCARMANT, AND EMMANUEL SAINT-CHRISTOPHE

***Abstract*—A three-wave recording interferometer has been modified in order to adapt it for the anisotropic measurements of rubber sheets**

Manuscript received April 4, 1989; October 23, 1989.
The authors are with the Laboratoire de Physique Expérimentale et des Microondes, Université de Bordeaux I, 351, Cours de la Libération, 33405 Talence, France.
IEEE Log Number 8933000.